7-1-1994

Statistics of the Scattering Cross Section of a Collection of Constant Amplitude Scatterers with Random Phase

Jihad S. Daba
Purdue University School of Electrical Engineering

Mark R. Bell
Purdue University School of Electrical Engineering

STATISTICS OF THE SCATTERING CROSS SECTION OF A COLLECTION OF CONSTANT AMPLITUDE SCATTERERS WITH RANDOM PHASE

JIHAD S. DABA
MARK R. BELL

TR-EE 94-25
JULY 1994

SCHOOL OF ELECTRICAL ENGINEERING
PURDUE UNIVERSITY
WEST LAFAYETTE, INDIANA 47907-1285

Statistics of the Scattering Cross Section of a Collection of Constant Amplitude Scatterers with Random Phase †

Jihad S. Daba and Mark R. Bell
School of Electrical Engineering
Purdue University
West Lafayette, IN 47907

†This work was supported by NSF Research Initiation Award MIP-9010834 and a David Ross Grant. A condensed version of this report has been submitted to the *IEEE Transactions on Antennas and Propagation.*

Abstract

Complex radar targets are often modeled as a number of individual scattering elements randomly distributed throughout the spatial region containing the target. While it is known that as the number of scatterers grows large, the distribution of the scattered signal power or intensity is asymptotically exponential, this is not true for a small number of scatterers. We study the statistics of measured power or intensity, and hence scattering cross section, resulting from a small number of constant amplitude scatterers, each having a random phase.

We first derive closed form expressions for the pdf of the scattered signal intensity, and then use an orthonormal series expansion for the pdf in terms of exponentially-weighted Laguerre polynomials when the number of scatterers is larger than 3. For the multilook case, an orthogonal series expansion in terms of Gamma-weighted generalized Laguerre polynomials is used to approximate the pdf.

The results of the Kolmogorov-Smirnov goodness-of-fit test show that the series expansions are a good fit to the actual pdfs.

1 Introduction

A common model for complex or extended radar targets is to consider them to consist of a collection of randomly distributed scattering elements [1]. Each scattering element making up the extended target is assumed to be a point target or isotropic scatterer, and each scattering element within the radar :resolution cell under consideration contributes a component to the total echo signal from that resolution cell. The statistics of the resulting radar cross section arising from the interfering scattered components from the target are difficult to derive. While the distribution of the energy scattered from a collection of Rayleigh scatterers or a collection of Rayleigh scatterers plus a constant scatterer can be easily derived [2], the statistical description of a fixed number of scatterers, with constant (nonrandom) amplitudes, randomly distributed in space, is not generally known. While it is known that for a large number of scatterers, the resulting scattering ensemble will exhibit Rayleigh scattering if a large number of elements are randomly scattered throughout a region whose dimensions are large compared to the wavelength of the illuminating radiation, this is not the case when the number of scatterers is small.

In this paper, we derive expressions for the probability distribution of the power or intensity of the scattered signal from, or equivalently the radar cross section of, a collection of constant scatterers randomly distributed in space within radar resolution cell. We first derive exact closed form expressions for the pdf of radar cross section arising from 1, 2, and 3 constant-amplitude scatterers based on a single look as a function of the scatterers amplitudes, using a recursive algorithm. We also derive an orthonormal series representation of the pdf in terms of exponentially-weighted Laguerre polynomials, when the number of scatterers within a resolution cell is greater than 3. For the multilook case, we obtain a closed form expression for the distribution of the sum of the intensities of each of the individual looks for 2 coherent scatterers based on 2 looks. For higher numbers of scatterers and looks, we expand the pdf as a series of Gamma-weighted orthogonal generalized Laguerre polynomials. Finally, we use the Kolmogorov-Srnirnov statistical test as a relative measure to determine how well the generalized Laguerre polynomial representation fits the actual pdf.

2 Scattering Cross Section Model

2.1 Single Look Model

In this model, a radar resolution cell is assumed to contain a collection of n elemental point scatterers randomly distributed throughout the resolution cell, with each elementary scatterer position distributed independently of the positions of other scatterers. For example, the elemental scatterers could be scatterers randomly distributed on a surface being imaged by an imaging radar and falling within the particular resolution cell of interest. Each backscattered electric field component E_j from the j-th scatterer, $j = 1, \ldots, n$, has a constant amplitude A_j equal to the size or reflectance strength of the j-th scatterer and a random phase ϕ_j uniformly distributed over the interval $[0, 2\pi)$:

$$E_j = A_j e^{i\phi_j}$$

The random phases of the elementary backscattered electric fields are also assumed to be statistically independent, because the random spatial locations of the individual scatterers are statistically independent. We assume that the number of elementary scatterers n is fixed, although n could in general be considered random, in which case the distributions we derive for fixed n would become condition.31intensity distributions conditioned on having the fixed number of scatterers within a

resolution cell. The superposition of the radar returns from each of the n elementary scatterers gives rise to the total backscattered electric field from the resolution cell as

$$\mathcal{M}_n = \sum_{j=1}^{n} \mathbf{E}_j. \tag{1}$$

The overall intensity measurement of the radar target is proportional to the square of the magnitude of $\mathcal{M}_n$ (intensity) given by

$$S_n = \left| \sum_{j=1}^{n} A_j e^{i\phi_j} \right|^2. \tag{2}$$

2.2 Multilook Model

In the multi-look model, L-independent diversity measurements are taken over the resolution cell by the radar. This technique involves the noncoherent sum of L statistically independent single realizations of the intensity measurements S_{nl} $(l = 1, 2, \ldots, \mathrm{L})$ in Eq. (2) at each resolution cell:

$$T_{nL} = \sum_{l=1}^{L} S_{nl}. \tag{3}$$

In SAR applications, this is a common technique for speckle reduction [3].

3 Probability Density Function of Single Look Intensity Measurement

3.1 Recursive Method

Figure 1 shows the geometry of the scattering problem we are examining, which can be described as a random walk of phasor components in the complex plane. Let the electric field reflected from the j-th elementary scatterer be denoted by

$$\mathbf{E}_j = A_j \mathrm{e}^{i\phi_j}, \tag{4}$$

where A_j is the scatterer amplitude assumed to be a fixed constant, and ϕ_j is its uniformly distributed random phase on the interval $[0, 2\pi)$. We also denote the electric field resulting from the coherent sum of k elementary scatterers by

$$\mathcal{M}_k = \sum_{j=1}^{k} \mathbf{E}_j, \tag{5}$$

and its magnitude by R_k for $k = 1, 2, \ldots, n$. We then have that the radar cross section $S_k = R_k^2$.

Assume that the intensity measurement S_{k-1} is known. We then can assume that the phase associated with $\mathcal{M}_{k-1}$ is zero, as indicated by the choice of reference in Fig. 1. We can write

$$\begin{aligned} S_k &= |R_{k-1} + A_k \mathrm{e}^{i\phi_k}|^2 && (6)\\ &= R_{k-1}^2 + A_k^2 + 2A_k R_{k-1} \cos(\phi_k) && (7)\\ &= A_k^2 + S_{k-1} + 2A_k \sqrt{S_{k-1}} \cos(\phi_k) && (8) \end{aligned}$$

The conditional cumulative distribution function of S_k conditioned on S_{k-1} can be written as

$$\begin{aligned} F_{S_k|S_{k-1}}(s_k|s_{k-1}) &= \Pr(S_k \le s_k | S_{k-1} = s_{k-1}) && (9)\\ &= \Pr\left(A_k^2 + s_{k-1} + 2A_k\sqrt{s_{k-1}}\cos(\phi_k) \le s_k\right) && (10)\\ &= 1 - \Pr\left(|\phi_k| > \cos^{-1}\left(\frac{s_k - A_k^2 - s_{k-1}}{2A_k\sqrt{s_{k-1}}}\right)\right) && (11)\\ &= 1 - \frac{1}{\pi}\arccos\left(\frac{s_k - A_k^2 - s_{k-1}}{2A_k\sqrt{s_{k-1}}}\right). && (12) \end{aligned}$$

Differentiating Eq. 12 with respect to s_k, we get the conditional pdf

$$p_{S_k|S_{k-1}}(s_k|s_{k-1}) = \begin{cases} \dfrac{1}{\pi\sqrt{\left((\sqrt{s_k}+A_k)^2 - s_{k-1}\right)\left(s_{k-1} - (\sqrt{s_k}-A_k)^2\right)}}, & (\sqrt{s_k}-A_k)^2 \le s_{k-1} \le (\sqrt{s_k}+A_k)^2 \\ 0, & \text{elsewhere.} \end{cases} \quad (13)$$

Using the Bayes' rule, the probability density function of S_k could be written as

$$p_{S_k}(s_k) = \int_0^\infty p_{S_k|S_{k-1}}(s_k|s_{k-1}) p_{S_{k-1}}(s_{k-1}) ds_{k-1}. \quad (14)$$

Hence, the probability density function of the intensity measurement S_n could be recursively determined by successive applications of Eqs. (13) and (14) for $k = 2, 3, \ldots, n$. In the following analysis we assume the relational order $A_{k-1} \le A_k$ for the scatterers amplitudes (k = 2, 3, . . . , n.)

3.1.1 Exact Probability Density Function for the Case of a Single Scatterer

When measurements are taken over a resolution cell consisting of a single scatterer, it is straightforward to show that $S_1 = A_1^2$, and hence

$$p_{S_1}(s_1) = \delta\left(s_1 - A_1^2\right), \quad (15)$$

where $\delta(\cdot)$ is the Dirac delta function.

3.1.2 Exact Probability Density Function for the Case of Two Scatterers

For the case when the resolution cell consists of 2 scatterers (n = 2), substituting Eqs. (15) and (13) into Eq. (14) (with k = 2) and applying the sifting property of the Dirac delta function yield

$$p_{S_2}(s_2) = \begin{cases} \dfrac{1}{\pi\sqrt{\left((\sqrt{s_2}+A_2)^2 - A_1^2\right)\left(A_1^2 - (\sqrt{s_2}-A_2)^2\right)}}, & (\sqrt{s_2}-A_2)^2 < A_1^2 < (\sqrt{s_2}+A_2)^2 \\ 0, & \text{elsewhere,} \end{cases} \quad (16)$$

or, after :replacing the constraint $(\sqrt{s_2} - A_2)^2 < A_1^2 < (\sqrt{s_2} + A_2)^2$ by its equivalent constraint $(A_1 - A_2)^2 < s_2 < (A_1 + A_2)^2$, and after some algebraic manipulations,

$$p_{S_2}(s_2) = \begin{cases} \dfrac{1}{\pi\sqrt{\left(s_2 - (A_1-A_2)^2\right)\left((A_1+A_2)^2 - s_2\right)}}, & (A_1 - A_2)^2 < s_2 < (A_1 + A_2)^2 \\ 0, & \text{elsewhere.} \end{cases} \quad (17)$$

The pdf $p_{S_2}(s_2)$ has singularities at $(A_1 - A_2)^2$ and $(A_1 + A_2)^2$. A plot of $p_{S_2}(s_2)$ is shown in Fig. 2, assuming unit amplitude scatterers ($A_1 = A2 + 1$).

3.1.3 Exact Probability Density Function for the Case of Three Scatterers

We now consider the case when the resolution cell consists of 3 scatterers (n = 3). Equation (14) is a convolution type integral. Thus, substituting Eqs. (17) and (13) into it (with k = 3) generates several cases depending on the relational order of the end points $(A_1-A_2)^2$, $(A_1+A_2)^2$, $(\sqrt{s_3}-A_3)^2$, and $(\sqrt{s_3}+A_3)^2$. For each case, the definite integral will take the general form

$$p_{S_3}(s_3) = \int_c^b \frac{1}{\pi^2\sqrt{(a-s_2)(b-s_2)(s_2-c)(s_2-d)}} ds_2, \quad (a>b>c>d) \tag{18}$$

where a, b, c, and d take on sets of values from the end points listed above.

In the first case, we assume that $(\sqrt{s_3}-A_3)^2 < (A_1-A_2)^2 < (A_1+A_2)^2 < (\sqrt{s_3}+A_3)^2$. Solving these inequalities for s_3 results in $(A_1-A2+A_3)^2 < s_3 < (-A_1+A_2+A_3)^2$. Also, a $= (\sqrt{s_3}+A_3)^2$, b $= (A_1+A_2)^2$, $c = (A_1-A_2)^2$, and d $= (\sqrt{s_3}-A_3)^2$.

In the second case, we assume that $(A_1-A_2)^2 < (\sqrt{s_3}-A_3)^2 < (\sqrt{s_3}+A_3)^2 < (A_1+A_2)^2$. We further assume that $A_3 \le A_1+A_2$. Solving for s_3 yields $0 \le s_3 < (A_1+A_2-A_3)^2$. We also have a $= (A_1+A_2)^2$, b $= (\sqrt{s_3}+A_3)^2$, c $= (\sqrt{s_3}-A_3)^2$, and d $= (A_1-A_2)^2$.

The third case arises when $(A_1-A_2)^2 < (\sqrt{s_3}-A_3)^2 < (A_1+A_2)^2 < (\sqrt{s_3}+A_3)^2$. Solving for s_3 gives the solution set

$$s_3 \in ((A_1+A_2-A_3)^2, (A_1-A_2+A_3)^2) \cup ((-A_1+A_2+A_3)^2, (A_1+A_2+A_3)^2).$$

For this case, a $= (\sqrt{s_3}+A_3)^2$, b $= (A_1+A_2)^2$, c $= (\sqrt{s_3}-A_3)^2$, and d $= (A_1-A_2)^2$.

The last case occurs when $(A_1-A_2)^2 < (A_1+A_2)^2 < (\sqrt{s_3}-A_3)^2 < (\sqrt{s_3}+A_3)^2$. This is equivalent to $s_3 \in [0,(A_1+A_2-A_3)^2) \cup ((A_1+A_2+A_3)^2, \infty)$ for $A_3 > A_1+A_2$, and $s_3 \in ((A_1+A_2+A_3)^2, \infty)$ for A3 $\le A_1+A_2$. The intervals $((A_1-A_2)^2, (A_1+A_2)^2)$ and $((\sqrt{s_3}-A_3)^2, (\&+\ A_3)^2)$ do not overlap. It follows that the pdf $p_{S_3}(s_3)$ is zero for this case.

The definite integral in Eq. (18), with a, b, c, and d in the given relational order, has the evaluation [4, p. 242]

$$p_{S_3}(s_3) = \frac{2}{\pi^2\sqrt{(a-c)(b-d)}} K(\chi), \tag{19}$$

where

$$\chi = \sqrt{\frac{(b-c)(a-d)}{(a-c)(b-d)}}, \tag{20}$$

and

$$K(\chi) = \int_0^{\pi/2} \frac{dy}{\sqrt{1-\chi^2\sin^2(y)}} \tag{21}$$

is the complete elliptic integral. Evaluating the expression in Eq. (19) for the different values that a, b, c, and d take in each of the above cases, and combining expressions for each interval s_3 takes on, yield the following closed form for the exact pdf:

$$p_{S_3}(s_3) = \begin{cases} 0, & 0 \le s_3 < (A_1+A_2-A_3)^2 \text{ for } A_3 > A_1+A_2 \\ \frac{2}{\pi^2 r(s_3)} K(q(s_3)), & 0 \le s_3 < (A_1+A_2-A_3)^2 \text{ for } A_3 \le A_1+A_2 \\ \frac{2}{\pi^2 t(s_3)} K(q^{-1}(s_3)), & (A_1+A2-A_3)^2 < s_3 < (A_1-A_2+A_3)^2 \\ \frac{2}{\pi^2 r(s_3)} K(q(s_3)), & (A_1-A2+A_3)^2 < s_3 < (-A_1+A_2+A_3)^2 \\ \frac{2}{\pi^2 t(s_3)} K(q^{-1}(s_3)), & (-A_1+A2+A_3)^2 < s_3 \le (A_1+A_2+A_3)^2 \\ 0, & s_3 > (A_1+A_2+A_3)^2 \end{cases} \tag{22}$$

where

$$t(s_3) = 4\sqrt{A_1 A_2 A_3 \sqrt{s_3}}, \tag{23}$$

$$r(s_3) = \sqrt{(\sqrt{s_3}+A_1+A_2-A_3)(\sqrt{s_3}+A_1-A_2+A_3)(\sqrt{s_3}-A_1+A_2+A_3)(-\sqrt{s_3}+A_1+A_2+A_3)}, \tag{24}$$

and

$$q(s_3) = \frac{t(s_3)}{r(s_3)}. \tag{25}$$

The pdf $p_{S_3}(s_3)$ has singularities at the end points $(A_1 + A_2 - A_3)^2$, $(A_1 - A2 + A_3)^2$, and $(-A_1 + A_2 + A_3)^2$. A graph of $p_{S_3}(s_3)$ is provided in Fig. 3, assuming unit-amplitude scatterers.

An exact closed form for the pdf of the intensity measurement S_n arising from **4** or more scatterers $(n \geq 4)$ is analytically intractable to derive using direct integration in Eq. (14). Developing a method of approximating this pdf for **4** or more scatterers is the topic of the next section.

3.2 Orthonormal Laguerre Polynomial Representation

3.2.1 Convergence to Rayleigh Scattering for Large number of Scatterers

Let us assume that the scatterers have equal amplitudes: $A_k = A_0$, for k = 1, 2, . . . , n. The in-phase and quadrature components of the total electric field $\mathcal{M}_n$ from the n scatterers are given by

$$\mathcal{M}_n^{(Re)} = \sum_{j=1}^{n} \mathbf{E}_j^{(Re)}$$

and

$$\mathcal{M}_n^{(Im)} = \sum_{j=1}^{n} \mathbf{E}_j^{(Im)},$$

respectively, where $\mathbf{E}_j^{(Re)} = A_j \cos(\phi_j)$ and $\mathbf{E}_j^{(Im)} = A_j \sin(\phi_j)$. The mean and variances of $\mathbf{E}_j^{(Re)}$ and $\mathbf{E}_j^{(Im)}$ are given by

$$\mathrm{E}\left(\mathbf{E}_j^{(Re)}\right) = \mathrm{E}\left(\mathbf{E}_j^{(Im)}\right) = 0,$$

and

$$\mathrm{Var}\left(\mathbf{E}_j^{(Re)}\right) = \mathrm{Var}\left(\mathbf{E}_j^{(Im)}\right) = A_0^2/2.$$

The central limit theorem states [5] that if $X_1, \ldots, X_n$ are independent and identically distributed random variables with mean μ and finite variance a^2, then the standardized random variable

$$Z_n = \frac{\sum_{j=1}^{n} X_j - n\mu}{\sqrt{n}\sigma}$$

is asymptotically Gaussian with zero mean and unit variance as $n \to \infty$. It follows then from the central limit theorem that $\mathcal{M}_n^{(Re)}$ and $\mathcal{M}_n^{(Im)}$ are both asymptotically Gaussian for n sufficiently large, each having mean zero and variance $nA_0^2/2$. It is also straightforward to show that $\mathrm{E}\left(M_n^{(Re)} M_n^{(Im)}\right) = E\left(M_n^{(Re)}\right) \mathrm{E}\left(\mathrm{M}_n^{(Im)}\right) = 0$, and so $M_n^{(Re)}$ and $\mathcal{M}_n^{(Im)}$ are uncorrelated Gaussian random variables, and hence independent.

A simple transformation rule yields the result that the intensity measurement $S_n = |\mathcal{M}_n^{(Re)} + i\mathcal{M}_n^{(Im)}|^2$ has an asymptotic exponential distribution of the form

$$p_{S_n}(s_n) \sim \frac{1}{\mathrm{n}A_0^2} \exp\left(-\frac{s_n}{nA_0^2}\right) I_{[0,\infty)}(s_n), \quad \text{for large } n, \tag{26}$$

where the indicator function $I_D(s)$ is defined as equal to 1 for $s \in$ D and 0 for $s \notin$ D. Thus, for a very large number n of scattering centers, the intensity measurement statistics converge to those of a Rayleigh scattering model.

3.2.2 Expansion of the PDF as a Series of Orthonormal Laguerre Polynomials

The pdf $p_{S_n}(s_n)$ was shown in the previous section to be asymptotically exponential. We use a Gram-Charlier type of expansion [6] and write $p_{S_n}(s,)$ as a series of exponentially weighted orthonormal Laguerre polynomials given by

$$p_{S_n}(s_n) \sim \frac{1}{nA_0^2} \exp\left(-\frac{s_n}{nA_0^2}\right) \left(1 + \sum_{m=1}^{M_n} c_m \mathcal{L}_m\left(\frac{s_n}{nA_0^2}\right)\right) I_{[0,\infty)}(s_n), \tag{27}$$

where $\mathcal{L}_m(s)$ are Laguerre polynomials [4, 7] defined by their expansion in powers of s:

$$\mathcal{L}_m(s) = \sum_{j=0}^{m} (-1)^j \binom{m}{m-j} \frac{s^j}{j!}. \tag{28}$$

The first few are: $\mathcal{L}_0(s) = 1, \mathcal{L}_1(s) = 1 - s, \mathcal{L}_2(s) = 1 - 2s + s^2/2$. The Laguerre polynomials obey the following orthogonality condition with respect to an exponential weighting function

$$\int_0^\infty \exp(-x)\mathcal{L}_m(x)\mathcal{L}_k(x)dx = \delta_{mk}, \tag{29}$$

where the Kronecker delta function δ_{mk} is defined as equal to 1 for m = k and 0 for m $\neq$ k.

The coefficients c_m measure the departure of the pdf $p_{S_n}(s,)$ from a pure exponential law, and are to be determined. Let us consider the expression

$$\begin{aligned}\int_0^\infty \left(p_{S_n}(x) - \frac{1}{nA_0^2}\exp\left(-\frac{x}{nA_0^2}\right)\right)\mathcal{L}_m\left(\frac{x}{nA_0^2}\right)dx &= \sum_{k=1}^{M_n} c_k \int_0^\infty \frac{1}{nA_0^2}\exp\left(-\frac{x}{nA_0^2}\right)\mathcal{L}_k\left(\frac{x}{nA_0^2}\right)\mathcal{L}_m\left(\frac{x}{nA_0^2}\right)dx \\ &= \sum_{k=1}^{M_n} c_k \delta_{km} \\ &= c_m,\end{aligned}$$

after applying the orthogonality condition of Eq. (29). Using the property [4]

$$\int_0^\infty \frac{1}{nA_0^2}\exp\left(-\frac{x}{nA_0^2}\right)\mathcal{L}_m\left(\frac{x}{nA_0^2}\right)dx = 0, \tag{30}$$

it follows that

$$c_m = \mathrm{E}\left(\mathcal{L}_m\left(\frac{s_n}{nA_0^2}\right)\right). \tag{31}$$

The expectation in Eq. (31) can be approximated using a maximum likelihood estimator **[8]** equal to the sample mean of a random sample of scattering cross sections $\{s_{nk}\}$:

$$\hat{c}_m = \frac{1}{K}\sum_{k=1}^{K} \mathcal{L}_m\left(\frac{s_{nk}}{nA_0^2}\right). \tag{32}$$

The intensity measurements $\{s_{nk}\}$, k = 1, 2, ..., K, are generated using computerized Monte Carlo simulation. Specifically, a pseudo-random number generator, employing the inverse distribution function method, is used to generate a large number (K = 1000) of statistically independent scattering ensembles made up of n unit-amplitude statistically independent random point scatterers with phases uniformly distributed over the interval $[0, 2\pi)$, according to Eq. (2). Table 1 shows the estimated coefficients $\hat{c}_m$ according to Eq. (32) for different numbers n of unit-amplitude scatterers ($A_0 = 1$).

The recursive expressions for the exact pdf in Eqs. (13) and (14) and the orthogonal series expansion in Eq. (27) were numerically implemented as Mathematica programs on a Sparc station for 4, 5, 6, 7, and **8** unit-amplitude scatterers. Table 2 gives the number of terms M_n (= M_{n1}) needed in the Laguerre expansion of the pdfs. Figure 4 illustrates the increasing exponential behavior of the pdf as the number of scatterers within a resolution cell is increased. The graphs of the exact pdfs versus their corresponding series expansions are illustrated in Figs. 5, 6, 7, and **8** for various numbers of scatterers n. The exact pdfs were numerically computed using the recursive integration method of section 3.1.

4 Probability Density Function of Multilook Intensity Measurements

In this section, we seek to develop a closed form expressions for the probability density function $p_{T_{nL}}(t_{nL})$ of the statistic T_{nL} given in Eq. (3) as the incoherent sum of L conditionally independent single realization intensity measurements ($\{S_{nl}\}, l = 1, 2, \ldots, L$).

4.1 Exact Probability Density Function for L-Look Intensity Measurement from a Single Scatterer

It is straightforward to show, using characteristic functions and (conditional) independence of the identically distributed single look intensity measurement, that the pdf of the statistic T_{nL} can be written as an L − 1 fold convolution [9]:

$$p_{T_{nL}}(t_{nL}) = p_{S_n}(t_{nL}) * p_{S_n}(t_{nL}) * \cdots * p_{S_n}(t_{nL}), \quad (L-1 \text{ fold}). \tag{33}$$

Substitution of Eq. (15) into Eq. (33) yields

$$p_{T_{1L}}(t_{1L}) = \delta(t_{1L} - A_1^2) * \delta(t_{1L} - A_1^2) * \ldots * \delta(t_{1L} - A_1^2), \quad (L-1 \text{ fold}) \tag{34}$$

or, after successive use of the sifting property of the Dirac delta function,

$$p_{T_{1L}}(t_{1L}) = \delta(t_{1L} - A_1^2 L). \tag{35}$$

4.2 Exact Probability Density Function for 2-Look Intensity Measurement from 2 Coherent Scatterers

Let us assume that the scatterers' amplitudes are ordered such that $A_1 \leq A_2$. The pdf of the statistic T_{nL} for 2-look intensity measurement arising from 2 scatterers (n = 2, L = 2) is the convolution of the pdf of a single look cross section from 2 scatterers with itself, as is readily verified by Eq. (33). Using the expression for the single look pdf $p_{S_2}(s_2)$ given in Eq. (17), we obtain

$$p_{T_{22}}(t_{22}) = \int_{t_{\min}}^{t_{\max}} \frac{1}{\pi^2 \sqrt{((A_1+A_2)^2-\tau)((t_{22}-(A_1-A_2)^2)-t_{22})(\tau-(A_1-A_2)^2)(\tau-(t_{22}-(A_1+A_2)^2))}}\, d\tau, \tag{36}$$

where $t_{\min}$ and $t_{\max}$ take on sets of values from the end points $(A_1-A_2)^2$, $(A_1+A_2)^2$, $t_{22}-(A_1+A_2)^2$, and $t_{22}-(A_1-A_2)^2$ depending on the relational order of these end points.

Equation (36) has the same form as Eq. (18) and can be evaluated using Eq. (19). Carrying on derivations identical to those in section 3.1.3 results in

$$p_{t_{22}}(t_{22}) = \begin{cases} 0, & t_{22} < 2(A_1-A_2)^2, \\ \frac{1}{2\pi^2} K(q(t_{22})), & t_{22} \in [2(A_1-A_2)^2, (A_1-A_2)^2+(A_1+A_2)^2) \\ & \quad \cup \left((A_1-A_2)^2+(A_1+A_2)^2, 2(A_1+A_2)^2\right], \\ 0, & t_{22} > 2(A_1+A_2)^2 \end{cases} \tag{37}$$

where

$$q(t_{22}) = \frac{1}{(A_1+A_2)^2-(A_1-A_2)^2} \sqrt{(t_{22}-2(A_1-A_2)^2)(2(A_1+A_2)^2-t_{22})}, \tag{38}$$

and $K(\cdot)$ is the complete elliptic integral defined in Eq. (21). The pdf has a singularity at the end point $(A_1-A_2)^2 + (A_1+A_2)^2$. Figure 9 illustrates the graph of $p_{t_{22}}(t_{22})$.

4.3 Orthogonal Generalized Laguerre Polynomial Representation

An exact closed form expression of the pdf of T_{nL} for n = 2, L $\geq$ 3 and n = 3, L $\geq$ 2 is not possible to derive by further application of the convolution in Eq. (33). Finding an orthogonal series approximation of the pdf is the topic of the next two sections.

4.3.1 Direct Method

The characteristic function of the l-th look intensity measurement S_{nl} ($l = 1, 2, \ldots, L$) is the Fourier transform of Eq. (27) evaluated at $-jw$ [10]:

$$\phi_{S_{nl}}(jw) \sim \frac{1}{n} \sum_{m=0}^{M_n} c_m \frac{(-jw)^m}{(-jw+\frac{1}{n})^{m+1}}. \tag{39}$$

Since $\{S_{nl}\}$ are i.i.d for all $1 = 1, 2, \ldots, L$, the characteristic function of T_{nL} is given by [9]

$$\phi_{T_{nL}}(jw) \sim (\phi_{S_{nl}}(jw))^L. \tag{40}$$

In Appendix A we show that applying an inverse Fourier transformation to Eq. (40) yields the pdf of T_{nL} as

$$p_{T_{nL}}(t_{nL}) \sim \frac{L!}{n^L} \sum_{(L_1,\ldots,L_{M_n+1}) \in S_L} \alpha_L \frac{(\nu_L-L)!}{(\nu_L-1)!} t_{nL}^{L-1} \exp\left(-\frac{t_{nL}}{n}\right) \mathcal{L}_{\nu_L-L}^{L-1}\left(\frac{t_{nL}}{n}\right) I_{[0,\infty)}(t_{nL}), \tag{41}$$

where

$$\alpha_L = \prod_{k=1}^{M_n+1} \left(\frac{c_{k-1}^{L_k}}{L_k!} \right), \tag{42}$$

$$\nu_L = \sum_{k=1}^{M_n+1} kL_k, \tag{43}$$

c_k is the k-th coefficient in the pdf expansion of the single look intensity measurement given by Eq. (27), and S_L is the set of all ordered (M, +1)-tuples of non negative integers whose sum is L. The functions $\mathcal{L}_m^\alpha(t)$ are the generalized Laguerre polynomials [4, 7] defined by

$$\mathcal{L}_m^\alpha(t) = \sum_{j=0}^{m} (-1)^j \binom{m+\alpha}{m-j} \frac{t^j}{j!}, \tag{44}$$

The first few are: $\mathcal{L}_0^\alpha(t) = 1, \mathcal{L}_1^\alpha(t) = 1+\alpha-t, \mathcal{L}_2^\alpha(t) = 1+(3/2)a+a^2/2-(2+a)t+t^2/2$. Note that $\mathcal{L}_m^0(t) = \mathcal{L}_m(t)$. The generalized Laguerre polynomials obey the following orthogonality condition with respect to a weighting gamma density function

$$\int_0^\infty x^\alpha \exp(-x) \mathcal{L}_m^\alpha(x) \mathcal{L}_k^\alpha(x) dx = \frac{\Gamma(\alpha+m+1)}{m!} \delta_{mk}, \tag{45}$$

where $\Gamma(\cdot)$ is the Gamma function defined as

$$\Gamma(\alpha) = \int_0^\infty t^{\alpha-1} \exp(-t) dt, \quad \alpha > 0. \tag{46}$$

For given n and L, the series expansion in Eq. (41) could always be rewritten, after regrouping terms, as a series of orthogonal generalized Laguerre polynomials weighted by a Gamma density function with parameters (L,n):

$$p_{T_{nL}}(t_{nL}) \sim \sum_{m=0}^{M} a_m \frac{1}{n^L \Gamma(L)} t_{nL}^{L-1} \exp\left(-\frac{t_{nL}}{n}\right) \mathcal{L}_m^{L-1}\left(\frac{t_{nL}}{n}\right) I_{[0,\infty)}(t_{nL}), \tag{47}$$

where a_m is a function of the coefficients c_m and the number of looks L. In Appendix B we provide an example illustrating the interpretation of Eq. (41) as a series of Gamma-weighted orthogonal generalized Laguerre polynomials.

The series coefficients a_m in Eq. (47) are obtained directly from the estimated coefficients $\hat{c}_m$ for the pdf expansion based on a single look. This makes the algorithm simpler to implement because intensity measurements simulations are not required to estimate the series coefficients, as in the single look case. The tradeoff, however, is an increased computational cost, since a relatively large number of series terms M is needed. For example, it is straightforward to show, following the example in Appendix B, that when the number of scatterers is 5 and the number of looks is 2, the resulting number of series terms M in Eq. (47) is equal to 14.

In the next section, we use a Gram-Charlier type of asymptotic expansion, and expand the pdf of T_{nL} as a series of orthogonal generalized Laguerre polynomials with arbitrary coefficients that do not depend on the estimated coefficients from the corresponding single look case. An estimation scheme is required to determine the series coefficients. However, the number of series terms required in the asymptotic expansion will be significantly lower than that in the direct approach method.

4.3.2 Asymptotic Expansion Method

The pdf of the l-th look intensity measurement S_{nl} was previously shown to be asymptotically exponential as in **Eq.** (26). It is readily shown, using characteristic functions [9], that the pdf of the statistic T_{nL} given in **Eq.** (3) has an asymptotic Gamma distribution with parameters (L, n) of the form

$$p_{T_{nL}}(t_{nL}) \sim \frac{1}{(nA_0^2)^L \Gamma(L)} t_{nL}^{L-1} \exp\left(-\frac{t_{nL}}{nA_0^2}\right) I_{[0,\infty)}(t_{nL}), \tag{48}$$

where A_0 is the common amplitude of the scatterers. Using a Gram-Charlier type of expansion, we then write $p_{T_{nL}}(t_{nL})$ as a series of Gamma weighted generalized Laguerre polynomials, given by

$$p_{T_{nL}}(t_{nL}) \sim \frac{1}{(nA_0^2)^L \Gamma(L)} t_{nL}^{L-1} \exp\left(-\frac{t_{nL}}{nA_0^2}\right) \left(1 + \sum_{m=1}^{M_{nL}} c_m \mathcal{L}_m^{L-1}\left(\frac{t_{nL}}{nA_0^2}\right)\right) I_{[0,\infty)}(t_{nL}). \tag{49}$$

Here c_m (not to be confused with the coefficients in **Eq.** (27)) measure the departure of the pdf from a pure Gamma law with parameters (L, n), and are to be determined. Multiplying both sides of **Eq.** (49) by $\mathcal{L}_k^{L-1}(t_{nL}/(nA_0^2))$, integrating with respect to t_{nL} over the interval [0,∞), applying the orthogonality condition of the generalized Laguerre polynomials of **Eq.** (45), and using the property [4, p. 845]

$$\int_0^\infty \frac{1}{(nA_0^2)^L \Gamma(L)} x^{L-1} \exp\left(-\frac{x}{nA_0^2}\right) \mathcal{L}_m^{L-1}\left(\frac{x}{nA_0^2}\right) dx = 0, \tag{50}$$

result in

$$c_m = \frac{1}{\binom{m}{m+L-1}} \mathrm{E}\left(\mathcal{L}_m^{L-1}\left(\frac{t_{nL}}{nA_0^2}\right)\right). \tag{51}$$

The derivation steps are identical to those shown in section 3.2.2.

We estimate the expectation above using the maximum likelihood sample rnean estimator

$$\hat{c}_m = \frac{1}{\binom{m}{m+L-1} K} \sum_{k=1}^{K} \mathcal{L}_m^{L-1}\left(\frac{t_{nL}^{(k)}}{nA_0^2}\right), \tag{52}$$

where $\{t_{nL}^{(k)}\}$ (k $= 1, 2, \ldots,$ K) are random samples from **Eq.** (3). Table **1** lists the estimated coefficients $\hat{c}_m$ obtained by generating 1000 random samples $\{t_{nL}^{(k)}\}$ through a Monte Carlo simulation method, for different numbers n of unit-amplitude scatterers ($A_0 = 1$) and different looks L.

Since an exact closed form expression for the pdf of T_{nL} for n $= 2,$ L ≥ 3 and n $= 3,$ L ≥ 2 is not known, we seek to estimate it using the Parzen window method [11]. We construct an estimator based on q random samples $\{t_{nL}^{(i)}\}(i = 1, 2, \ldots, q)$ from the probability density function. The estimator has the form

$$\hat{p}_{T_{nL}}(t_{nL}) = \frac{1}{q} \sum_{i=1}^{q} \frac{1}{h_q} \phi\left(\frac{t_{nL} - t_{nL}^{(i)}}{h_q}\right), \tag{53}$$

where

$$\phi(t) = \frac{1}{\sqrt{2\pi}} \exp\left(-\frac{t^2}{2}\right) \tag{54}$$

is a Gaussian window function, and $h_q = h_1/\sqrt{q}$, with h_1 acting as a smoothing factor for the estimated curve. A very small h_1 causes the estimate to suffer from too much statistical fluctuation.

On the other hand, a very large value of h_1 causes the estimate to suffer from too little resolution, and thus requires a larger number of samples q to be generated [11].

For the purpose of comparing the estimated pdfs with the series expansion approximations, we generated a large number q of random samples $\{t_{nL}^{(i)}\}$ using Eqs. (2) and (3) and form the estimated pdf from Eq. (53). We use the values of q = 100,000 and $h_1 = 100$ in the Parzen density estimation. These values enabled us to obtain estimates of both sufficiently high resolution and negligible statistical fluctuation.

Figure 10 shows that the pdf (estimated) approaches a Gamma density function as the number of scatterers increases for a fixed number of looks (L = 2). On the other hand, Figs. 11 shows that the pdf also approaches a Gamma distribution as the number of looks L is increased for fixed numbers of scatterers (n = **2).**

Figures 12–17 provide plots of the pdf's orthogonal expansion given in **Eq.** (49) against the pdf estimated through the Parzen window algorithm for various numbers n of unit-amplitude scatterers and different numbers of looks L. The numbers of series terms M_{nL} are listed in Table 2. We mentioned in the previous section that for n = 5 and L = 2, 14 series terms were needed in the expansion given in Eq. (47). Table 2 indicates that only 3 series terms are needed in the asymptotic expansion approach. This shows the computational advantage of the asymptotic expansion method over the direct method studied in the previous section, and that it is worthwhile estimating the series coefficients rather than obtaining them directly from the series coefficients of the corresponding single look case.

Kolmogorov-Smirnov "Goodness-of-Fit" Test

The Kolmogorov-Smirnov statistical test [12, 13, 14] described below, provides a quantitative method to determine how well the orthogonal series approximation of the pdf in terms of Laguerre (or generalized Laguerre) polynomials fits the actual pdf.

5.1 Test Description

Let $\{X_k\}$, k = 1, 2, . . . , K, be a random sample of K independent identically distributed random variables from a continuous cumulative distribution $F(x)$ on the interval [0,∞). The Kolmogorov-Smirnov test is used to test the hypothesis that the samples $\{X_k\}$ come from $F(x)$. We form the order statistics $X_{(1)}, \ldots, X_{(K)}$ corresponding to the random sample $X_1, \ldots, X_K$, and we then construct the sample distribution

$$F_K(x) = \begin{cases} 0, & \text{for } x < X_{(1)}, \\ j/K, & \text{for } X_{(j)} \le x < X_{(j+1)}, \ (j = 1, \ldots, K-1) \\ 1, & \text{for } x \ge X_{(K)}. \end{cases} \tag{55}$$

The distance metric between the sample distribution $F_K(x)$ and the actual distribution $F(x)$ defined as

$$D_K(X_1, \ldots, X_K) = \sup_x |F_K(x) - F(x)|, \tag{56}$$

will be used to test the hypothesis. If D_K is less than a threshold rp chosen to give a test of desired confidence level β (probability of accepting the hypothesis when it is true), we accept the hypothesis. If D_K exceeds the value rp, we reject the hypothesis. The value of rp for a given β is

the solution to the equation

$$\Pr(D_K \leq r_\beta) = 1 - 2\sum_{i=1}^{\infty}(-1)^{i-1}\exp\left(-2Ki^2r_\beta^2\right) = \beta. \tag{57}$$

The value of $r_\beta = 0.07279$ for a 99% confidence level using Eq. (57) and 500 random samples.

5.2 Test Application

The computation of the cumulative distributions of the single look and multilook intensity measurements by direct integration of Eqs. (27) and (49), respectively, is computationally inefficient. We thus seek to derive closed form expressions for the cumulative distributions.

The cumulative distribution of the single look intensity measurement is given by

$$F(s_n) = \frac{1}{nA_0^2}\int_0^{s_n}\exp\left(-\frac{x}{nA_0^2}\right)dx + \sum_{m=1}^{M_n} c_m \frac{1}{nA_0^2}\int_0^{s_n}\exp\left(-\frac{x}{nA_0^2}\right)\mathcal{L}_m\left(\frac{x}{nA_0^2}\right)dx. \tag{58}$$

The above expression has the evaluation [4, p. 844]

$$F(s_n) = 1 - \exp\left(-\frac{x}{nA_0^2}\right)\left(1 + \sum_{m=1}^{M_n} c_m\left(\mathcal{L}_m\left(\frac{x}{nA_0^2}\right) - \mathcal{L}_{m-1}\left(\frac{x}{nA_0^2}\right)\right)\right). \tag{59}$$

We form the cumulative distribution of the multilook intensity measuremerit as

$$\begin{aligned} F(t_{nL}) &= \frac{1}{\Gamma(L)(nA_0^2)^L}\int_0^{t_{nL}} x^{L-1}\exp\left(-\tfrac{x}{nA_0^2}\right)dx + \frac{1}{\Gamma(L)(nA_0^2)^L} \\ &\quad \cdot \sum_{m=1}^{M_{nL}} c_m \int_0^{t_{nL}} x^{L-1}\exp\left(-\tfrac{x}{nA_0^2}\right)\mathcal{L}_m^{L-1}\left(\tfrac{x}{nA_0^2}\right)dx. \end{aligned} \tag{60}$$

Successive integrations by parts yield the following closed form expression:

$$\begin{aligned} F(t_{nL}) &= 1 - Q_L\left(0, \sqrt{\tfrac{2t_{nL}}{nA_0^2}}\right) + \frac{\exp\left(-\frac{t_{nL}}{nA_0^2}\right)}{\Gamma(L)}\sum_{m=1}^{M_{nL}} c_m \sum_{l=1}^{L}(-1)^l(1-L)_{l-1}\left(\tfrac{t_{nL}}{nA_0^2}\right)^{L-l} \\ &\quad \cdot \sum_{k=0}^{l}(-1)^k\binom{l}{k}\mathcal{L}_{m-k}^{L-1}\left(\tfrac{t_{nL}}{nA_0^2}\right), \end{aligned} \tag{61}$$

where the function $Q_L(0,x)$ is the generalized Marcum Q-function [15] defined as

$$Q_L(0,x) = \exp\left(-\frac{x^2}{2}\right)\sum_{l=0}^{L-1}\frac{x^{2l}}{2^l l!}. \tag{62}$$

The notation $(1-L)_{l-1}$ is the Pochhammer symbol defined by $(\alpha)_0 = 1$ and

$$(\alpha)_j = \prod_{i=0}^{j-1}(\alpha + i), \quad \text{for } j \neq 0. \tag{63}$$

The derivation of Eq. (61) is deferred to Appendix C.

Having derived closed form expressions for the cumulative distribution of the intensity measurement, we compute the distance D_K using Eq. (56). For simplicity, we assume that the scatterers have unit-amplitudes ($A_0 = 1$). Figures 18–20 illustrate the distance between the intensity measurement distribution and the sample distribution as a function of the number of series terms, for various numbers of scatterers and looks. The distances are also compared with the threshold of the 99% confidence level. Each graph was constructed using 500 intensity measurements simulations.

6 Results and Discussion

6.1 Probability Density of Intensity Measurement for Single Look Case

For single look intensity measurement, we note that the exact pdf approaches an exponential distribution as the number of the scatterers is gradually increased from 4 to 7, as illustrated in Figs. 4–8 For the case of 4 scatterers, a relatively high number of series terms ($M_{nL} = 17$) is needed to approximate the pdf up to a 5% maximum relative error. An increase in the number of terms M_{nL} to 20 or 25 merely reduces the maximum relative error to 4%. It takes as many as 35 terms to obtain a significantly lower maximum relative error of 2% at the cost of increasing the computational complexity of the Laguerre polynomial expansion. Considering the trade off between computational complexity and relative error, we use only 17 terms in the series expansion and accept an increased maximum relative error of 5%. Increasing the number of scatterers from 4 to only 5 scatterers significantly reduces the number of series terms from 17 to 7, while maintaining a maximum relative error of 5%. As the number of scatterers is further increased to 6 and 7 scatterers, the pdfs converge faster to an exponential distribution and only 3 and 2 series terms are needed, respectively, for a remarkably low maximum relative error of 2%. Furthermore, the graph of the Laguerre series expansion is almost indistinguishable from the exact pdf for the case of 7 scatterers. Only one series term is needed for the case of 8 scatterers to maintain a maximum relative error of 2%. For 9 or more scatterers, the central limit theorem (section 3.2.1) applies, M_{nL} is taken to be zero, and the exponential law of Eq. (26) is used to represent the pdf.

6.2 F'robability Density of Intensity Measurement for Multilook Case

For multilook intensity measurement, Fig. 10 shows that the pdf (estimated) approaches a Gamma density function as the number of scatterers is increased from 2 to 5 for a fixed number of looks (L = 2). Figure 11 illustrates that the pdf also approaches a Gamma distribution as the number of looks is increased from 2 to 5 for fixed numbers of scatterers (n = 2). This means that the effect of adding up L intensity measurements from a fixed number of scatterers within a resolution cell on the pdf behavior is the same as increasing the number of scatterers with the resolution cell for a lower number L of looks.

Notice from Table 2 that the number of terms M_{nL} used in the orthogonal series representation of the pdf drops at a faster rate by increasing n for a fixed L than it does by increasing L for a fixed n. For example, assuming the resolution cell consists of 2 scatterers, an increase in the number of looks from 4 to 5 causes the number of series terms M_{nL} to drop from 14 to only 10. On the other hand, assuming 2 looks are taken, a small increase in the number of scatterers from 4 to 5 causes M_{nL} to drop significantly from 12 to 3.

For a very low number of looks, the numerical implementation of the generalized Laguerre polynomial representation of the pdf may not be computationally efficient, since a relatively high number of series terms is needed when the number of scatters within a resolution cell is very small (on the order of 2 or 3). However, the series implementation could be rendered highly efficient by increasing the number of looks to only 4. In this case, the largest number of series terms needed is only 5, excluding the case when n = 2. Even if n = 2, the number of looks could be increased to only 6, and the number of series terms will be at most 6.

6.3 The Kolmogorov-Smirnov Test's Interpretation

The distance D_K associated with the Kolrnogorov-Smirnov test is used as a relative measure to determine how well the generalized Laguerre polynomial representation of the pdf fits a large number of simulated intensity observations from the measurement Equations (2) and (3).

In Fig. 18, D_K is plotted against the number of series terms M_n as the number of scatterers increases from 4 to 7 for a fixed single look. We notice that the distances are always below the threshold $r_{99\%} = 0.07279$ for all n. Thus D_K for the simulated scatterer ensembles falls below the threshold that 99% of all random samples made up of 500 intensity measurements actually drawn from the series expansion pdf would fall. (For the purpose of comparison, we note that the corresponding 50% and and 95% thresholds are $r_{50\%} = 0.03701$ and $r_{95\%} = 0.06074$). In general, when the D_K associated with a random sample is less than the threshold $r_{99\%}$, it is reasonable to assume that the random sample actually came from the hypothesized series expansion pdf, as the maximum absolute deviation between the empirical distribution obtained from the random sample and the hypothesized distribution is quite small. For n = 6 and 7, we notice that the distance remains relatively constant for $M_n \geq 5$. Thus, adding more terms in the series will not make a significant improvement in the representation of the pdf. For n = 5, the drops in the distance values are noticeable only as M_n is increased to 7. On the other hand, for the case when n = 4, it takes as much as 18 terms before the drops in distance values become insignificant. These values of the series terms are consistent, on a magnitude order, with those obtained analytically and listed in Table 2.

Figure 19 illustrates the graphs of D_K as n increases from 3 to 5 for 2 looks. Again we note that the graphs are below the threshold for all n. We also note that as n is varied from 3 to 5, the drops in the values of D_K become insignificant after 14, 10, and 3 terms, respectively. These values of M_{nL} are of the same magnitude as those listed in Table 2.

Figure 20 provides a graph of D_K as the number of looks is increased for a fixed n. It is noted that the distances are below the threshold level for all L. In addition, the values of the series terms M_{nL} above which the distances remain relatively constant agree in magnitude with the ones listed in Table 2.

Using the Kolmogorov-Smirnov statistical test, we conclude that the orthogonal series representation of the pdf is a good fit to the actual pdf, given the values of the series terms listed in Table 2.

7 Summary and Conclusions

In this paper, we investigated the statistics of intensity measurements, and hence scattering cross section of constant-amplitude scatterers. We first derived exact closed form expressions for the intensity':; pdf as a function of the scatterers' constant amplitudes, when the number of scatterers within a resolution cell is 1, 2, and 3, and a single look is taken over the resolution cell. It was noted from the graphs of the pdf obtained by numerical implementation of the recursive algorithm that the pdf approached an exponential distribution as the number of scatterers was increased. When the number of scatterers within a resolution cell was greater than 3, we used a Gram-Charlier type of expansion and represented the pdf as an orthonormal series of exponentially-weighted Laguerre polynomials. The series coefficients were estimated using a maximum likelihootl estimator and the number of series terms were tabulated.

Next, we studied the probability density of intensity measurements based on L looks. An exact closed form expression for the pdf of the L-look intensity arising from a single scatterer and 2-look intensity arising from 2 coherent scatterers was derived. For higher numbers of scatterers and looks,

we estimated the pdf using the Parzen window method, and noticed that the pdf approached a Gamma density function as the number of looks was increased for a fixed number of scatterers. The pdf also approached a Gamma density at a faster rate when the number of scatterers was increased for a fixed number of looks. This motivated the use of a Gram-Charlier type of expansion to approximate the pdf as an orthogonal series of Gamma-weighted generalized Laguerre polynomials. The series coefficients were then estimated using a maximum likelihood estimator, and the number of series terms were also tabulated. We found that for 4 or more looks, the number of series terms needed in the expansion was very small (at most 5), even when the resolution cell consists of only 3 scatterers. If the number of scatterers is as low as 2, the number of looks could be increased to only 6 in order to obtain a low number of series terms equal to 6. Hence, the numerical implementation of the series representation of the pdf that we presented is highly efficient.

Finally, we derived closed form expressions for the cumulative distribution functions of the intensity. The metric distance between the intensity distribution corresponding to the asymptotic expansion of the pdf and the sample pdf constructed based on 500 simulated random intensity samples was used as a relative measure in the Kolmogorov-Smirnov statistical test to determine how well the asymptotic expansion fits the actual pdf. The distance was plotted against the number of series terms for various cases of looks and numbers of scatterers. We noted from the graphs that the distances were below the threshold of the 99% confidence level for all values of n and L considered. We also noted that the distances remained relatively constant after certain values of series terms. These values were consistent, on a magnitude order, with those obtained analytically.

We conclude that the series expansions of the pdf in terms of generalized Laguerre polynomials are a good representation of the actual pdf.

We expect the pdf expressions and approximations derived in this paper to be useful in extraction and estimation of surface roughness information from radar measurements of surfaces whose scattering; characteristics are dominated by a relatively small number of scatterers per resolution cell. Specifically, the closed form expressions derived for the probability density function of the intensity and their associated orthogonal series expansions will be the key to formulating parametric estimators to determine the surface reflectivity of SAR images from partially developed speckle measurements.

A Derivation of the Generalized Laguerre Series Expansion of Equation (41)

From Eqs.(39) and (40), the characteristic function of T_{nL} takes the form:

$$\phi_{T_{nL}}(jw) \sim \frac{1}{n^L}\left(\sum_{m=0}^{M_n} c_m \frac{(-jw)^m}{(-jw+\frac{1}{n})^{m+1}}\right)^L . \tag{64}$$

Using the multinomial formula [16] yields

$$\phi_{T_{nL}}(jw) \sim \frac{L!}{n^L} \sum_{(L_1,\ldots,L_{M_n+1})\in S_L} \left(\prod_{k=1}^{M_n+1}\left(\frac{c_{k-1}^{L_k}}{L_k!}\right)\right) \frac{(jw)^{(\sum_{k=1}^{M_n+1} kL_k)-L}}{(jw+\frac{1}{n})^{\sum_{k=1}^{M_n+1} kL_k}}, \tag{65}$$

where S_L is the set of all (M_n+1)-tuples of non negative integers whose sum is L. The pdf of T_{nL} is the inverse Fourier transformation of its characteristic function [9], as in

$$p_{T_{nL}}(t_{nL}) \sim \frac{L!}{n^L} \sum_{(L_1,\ldots,L_{M_n+1})\in S_L} \left(\prod_{k=1}^{M_n+1} \left(\frac{c_{k-1}^{L_k}}{L_k!} \right) \right) \mathcal{F}^{-1} \left\{ \frac{(jw)^{\left(\sum_{k=1}^{M_n+1} kL_k\right)-L}}{\left(jw+\frac{1}{n}\right)^{\sum_{k=1}^{M_n+1} kL_k}} \right\}. \tag{66}$$

Setting

$$\alpha_L = \prod_{k=1}^{M_n+1} \left(\frac{c_{k-1}^{L_k}}{L_k!} \right), \tag{67}$$

and

$$\nu_L = \sum_{k=1}^{M_n+1} kL_k, \tag{68}$$

and using: inverse Laplace transformation tables (after mapping jw in the Fourier domain to p in the Laplace domain) [17] yields the result

$$p_{T_{nL}}(t_{nL}) \sim \frac{L!}{n^L} \sum_{(L_1,\ldots,L_{M_n+1})\in S_L} \alpha_L \frac{(\nu_L-L)!}{(\nu_L-1)!} t_{nL}^{L-1} \exp\left(-\frac{t_{nL}}{n}\right) \mathcal{L}_{\nu_L-L}^{L-1}\left(\frac{t_{nL}}{n}\right) I_{[0,\infty)}(t_{nL}). \tag{69}$$

B Interpretation of Equation (41) as a Series of Orthogonal Generalized Laguerre Polynomials

Let us consider the case of *8* scatterers and *3* looks *(n= 8, L = 3)*. Table *2* shows that only one term is needed in the series expansion of the intensity's pdf based on a single look *($M_n = 1$)*. For this example, the set S_L of ordered pairs (L_1, L_2) in Eq. *(41)* is given by $S_L = \{(3,0),(2,1),(1,2),(0,3)\}$. To each cadered pair (L_1, L_2) in S_L there corresponds different numbers α_L and ν_L as defined in Eqs. *(42)* and *(43)*.

Let A_ν denote the set of numbers $\nu_L - L$ and B_α denote the set of numbers α_L corresponding to each pair (L_1, L_2) in S_L. For this specific set, we have $A_\nu = \{0,1,2,3\}$ and $B_\alpha = \{1/6, c_1/2, c_1^2/2, c_1^3/6\}$. Let $M = card(B_\alpha) - 1 = 3$ ($card(D)$ is the cardinal of the set D). We also denote the m-th element of the set B_α by $(B_\alpha)_m$, m = 0, 1, ..., M. Hence, we can rewrite the sum in Eq. *(41)* over the set S_L as

$$p_{T_{nL}}(t_{nL}) \sim \sum_{m=0}^{M} a_m \frac{1}{n^L \Gamma(L)} t_{nL}^{L-1} \exp\left(-\frac{t_{nL}}{n}\right) \mathcal{L}_m^{L-1}\left(\frac{t_{nL}}{n}\right) I_{[0,\infty)}(t_{nL}), \tag{70}$$

where

$$a_m = \frac{L!}{\binom{m+L-1}{m}} (B_\alpha)_m .$$

C Derivation of the Cumulative Distribution of the Multilook Intensity (Eq. (61))

Consider the definite integral

$$\psi_1(t_{nL}) = \frac{1}{\Gamma(L)(nA_0^2)^L} \int_0^{t_{nL}} x^{L-1} \exp\left(-\frac{x}{nA_0^2}\right) dx. \tag{71}$$

Successive integrations by parts result in

$$\psi_1(t_{nL}) = 1 - Q_L\left(0, \sqrt{\frac{2t_{nL}}{nA_0^2}}\right), \tag{72}$$

where $Q_L(0, \mathrm{x})$ is the generalized Marcum Q-function.

Now, let us examine the definite integral

$$\psi_2(t_{nL}) = \frac{1}{\Gamma(L)(nA_0^2)^L} \int_0^{t_{nL}} \mathrm{x}^{L-1} \exp\left(-\frac{x}{nA_0^2}\right) \mathcal{L}_m^{L-1}\left(\frac{x}{nA_0^2}\right) dx. \tag{73}$$

A simple change of variable yields

$$\psi_2(t_{nL}) = -\frac{1}{\Gamma(L)} \int_{\frac{t_{nL}}{nA_0^2}}^{\infty} y^{L-1} \exp(-y) \mathcal{L}_m^{L-1}(y) dy. \tag{74}$$

Applying successive integrations by parts, by induction, we will show that

$$\begin{aligned} \int_x^{\infty} y^{L-1} \exp(-y) \mathcal{L}_m^{L-1}(y) dy \;&=\; \exp(-x) \sum_{l=1}^{L} (-1)^{l-1} (1-L)_{l-1} x^{L-l} \\ &\quad \cdot \sum_{k=0}^{l} (-1)^k \binom{l}{k} \mathcal{L}_{m-k}^{L-1}(x), \end{aligned} \tag{75}$$

where $\mathrm{x} = t_{nL}/(nA_0^2)$. We now prove Eq. (75) for $\mathrm{L} \geq 1$ by induction.

For $\mathrm{L} = 1$, the left hand side of **Eq.** (75) becomes [4, p. 844]

$$\mathrm{LHS} = \int_x^{\infty} \exp(-y) \mathcal{L}_m^0(y) dy = exp(-x) \left(\mathcal{L}_m(x) - \mathcal{L}_{m-1}(\mathrm{x})\right). \tag{76}$$

The right hand side of **Eq.** (75) simplifies to

$$\mathrm{RHS} = \exp(-x) \sum_{k=0}^{1} (-1)^k \binom{1}{k} \mathcal{L}_{m-k}^0(x) = exp(-x) \left(\mathcal{L}_m(x) - \mathcal{L}_{m-1}(x)\right). \tag{77}$$

Thus, **Eq.** (75) is verified for $\mathrm{L} = 1$.

Now, 'let us assume that **Eq.** (75) is true for L (hypothesis of induction). We need to prove that it is true for $\mathrm{L} + 1$. For $\mathrm{L} + 1$, the left hand side of **Eq.** (75) is

$$\mathrm{LHS} = \int_x^{\infty} y^L \exp(-y) \mathcal{L}_m^L(y) dy = \int_x^{\infty} y^{L-1} \exp(-y) \left(y \mathcal{L}_m^L(y)\right) dy, \tag{78}$$

or, using the functional relation [4, p. 1037]

$$y\mathcal{L}_m^L(y) = (m+L)\mathcal{L}_m^{L-1}(y) - (m+1)\mathcal{L}_{m+1}^{L-1}(y), \tag{79}$$

$$\text{LHS} = (m+L)\int_x^\infty y^{L-1}\exp(-y)\mathcal{L}_m^{L-1}(y)dy - (m+1)\int_x^\infty y^{L-1}\exp(-y)\mathcal{L}_{m+1}^{L-1}(y)dy. \tag{80}$$

Applying the hypothesis of induction, we obtain

$$\begin{aligned}\text{LHS} &= (m+L)\exp(-x)\sum_{l=1}^{L}(-1)^{l-1}(1-L)_{l-1}x^{L-l}\sum_{k=0}^{l}(-1)^k\binom{l}{k}\mathcal{L}_{m-k}^{L-1}(x)\\ &\quad -(m+1)\exp(-x)\sum_{l=1}^{L}(-1)^{l-1}(1-L)_{l-1}x^{L-l}\sum_{k=0}^{l}(-1)^k\binom{l}{k}\mathcal{L}_{m-k}^{L-1}(x).\end{aligned} \tag{81}$$

Successive use of the functional relations [4, p. 1037]

$$\mathcal{L}_m^{L-1}(x) = \mathcal{L}_m^L(x) - \mathcal{L}_{m-1}^L(x), \tag{82}$$

and

$$(\mathrm{m}+1)\mathcal{L}_{m+1}^L(x) - (2\mathrm{m}+\mathrm{L}+1-x)\mathcal{L}_m^L(x) + (m+L)\mathcal{L}_{m-1}^L(x) = 0, \tag{83}$$

and regrouping terms, yield the RHS of Eq. (75) for L + 1. This concludes the proof of Eq. (75).

Substituting Eqs. (72), (74), and (75) into Eq.(60) results in

$$\begin{aligned}F(t_{nL}) &= 1 - Q_L\left(0, \sqrt{\tfrac{2t_{nL}}{nA_0^2}}\right) + \frac{\exp\left(-\frac{t_{nL}}{nA_0^2}\right)}{\Gamma(L)}\sum_{m=1}^{M_{nL}}c_m\sum_{l=1}^{L}(-1)^l(1-L)_{l-1}\left(\tfrac{t_{nL}}{nA_0^2}\right)^{L-l}\\ &\quad \cdot\sum_{k=0}^{l}(-1)^k\binom{l}{k}\mathcal{L}_{m-k}^{L-1}\left(\tfrac{t_{nL}}{nA_0^2}\right).\end{aligned} \tag{84}$$

References

[1] R. V. Ostrovityanov and F. A. Basalov, Statistical Theory of Extended Radar Targets, Dedham, MA: Artech House, 1985.

[2] S. O. Rice, "Mathematical Analysis of Random Noise," Bell Sys. Tech. Journal, vol. 23, pp. 282–352, and vol. 24, pp. 46–156,

[3] J. W. Goodman, "Statistical Properties of Laser Speckle Patterns," Laser Speckle and Related Phenomena, 2d. ed., ed. J. C. Dainty, New York, NY: Springer-Verlag, 19134.

[4] I. S. Gradsheyten and I. M. Ryzhik, Tables of Integrals, Series, and Products, New York, NY: Academic Press, Inc., 1980.

[5] E. B. Manoukian, Modern Concepts and Theorems of Mathematical Statistics, New York, NY: Springer-Verlag, 1986.

[6] B. R.. Frieden, Probability, Statistical Optics, and Data Testing, New York, NY: Springer-Verlag, 1991.

[7] V. S. Aizenshtadt, V. I. Krylov, and A. S. Metel'skii, Tables of Laguerre Polynomials and Functions, New York, NY: Pergamon Press, 1966.

[8] L. L. Scharf, Statistical *Signal* Processing, New York, NY: Addison-Wesley, 1990.

[9] A. F'apoulis, Probability, Random Variables, and Stochastic Processes, 3rd ed., New York, NY: McGraw-Hill, 1991.

[10] A. P. Prodnikov, Yu. A. Brychkov, O. I. Marichu, Integral and Series: Direct *Laplace Trans*form, Philadelphia, PA: Gordon and Breach Science Publishers, Vol. 4, 1992.

[11] R. Duda and P. Hart, Pattern Classification and Scene Analysis, New York, NY: Wiley-Interscience, 1973.

[12] A. N. Kolmogorov, "Sulla determinazione empirica di una legge di distribuzione," Ist. Ital. Attuari., G, Vol. 4, pp. 1-11, 1933. English translation in Breakthroughs in *Statistics*, Volume II, S. Kotz and N. L. Johnson, eds., New York, NY: Springer-Verlag, 1991.

[13] F. J. Massey, "The Kolmogorov-Smirnov tests for goodness of fit," J. Amer. Stat. Assoc., Vol. 46, pp. 68–78, 1951.

[14] H. Lilliefors, "On the Kolmogorov-Smirnov test for normality with mean and variance unknown," J. Amer. Stat. Assoc., Vol. 62, pp. 399–402, 1967.

[15] D. A. Shnidman, "The calculation of the probability of detection and the generalized Marcum Q-function," IEEE *Trans.* Info. Theory, Vol. 35, No. 2, pp. 389–400, 1989.

[16] M. R.. Spiegel, Mathematical Handbook of Formulas and Tables, New York, NY: McGraw-Hill, 1990.

[17] A. P. Prodnikov, Yu. A. Brychkov, O. I. Marichu, Integral and Series: *Inverse Laplace Trans*form, Philadelphia, PA: Gordon and Breach Science Publishers, Vol. 5, 1992.

Table 1: Values of the estimated coefficients $\hat{c}_m$ in the (Generalized) Laguerre polynomial expansion for unit-amplitude scatterers.

L	m	n 3	4	5	6	7	8
1	1		1.072033-04	4.417223-04	-1.590983-04	-3.00960E-04	8.013013-04
	2		-1.248863-01	-1.002323-01	-8.344113-02	-7.11855E-02	
	3		-4.20834E-02	-2.658073-02	-1.824793-02		
	4		2.505613-02	1.95443E-02			
	5		3.746663-02	2.131313-02			
	6		1.592543-02	4.440573-03			
	7		-1.090513-02	-8.352883-03			
	8		-2.597253-02				
	9		-2.343293-02				
	10		-7.927003-03				
	11		1.369163-02				
	12		3.465153-02				
	13		4.955303-02				
	14		5.58110E-02				
	15		5.421843-02				
	16		4.560103-02				
	17		3.30694E-02				
2	1	-3.033893-04	-5.122873-04	3.850483-05	-5.60070443-05		
	2	-1.11143E-01	-8.309133-02	-6.644743-02			
	3	-3.678523-02	-2.125733-02	-1.337203-02			
	4	1.826253-02	1.348483-02				
	5	2.951313-02	1.409443-02				
	6	1.599723-02	3.823033-03				
	7	-2.582813-03	-4.325043-03				
	8	-1.562983-02	-6.553533-03				
	9	-2.108283-02	-4.284383-03				

Table 1: (continued)

L	m	n 2	3	4	5
2	10		-2.08613E-02	-6.09230E-04	
	11		-1.72613E-02	3.11385E-03	
	12		-1.29405E-02	5.44684E-03	
	13		-8.44614E-03		
	14		-4.80857E-03		
	15		-1.91516E-03		
	16		2.71963E-04		
	17		2.08414E-03		
3	1	-7.40026E-05	-5.96712E-05	2.49152E-04	-1.95004E-04
	2	-1.24986E-01	-8.33289E-02	-6.25077E-02	
	3	-4.98627E-02	-2.22484E-02	-1.24521E-02	
	4	1.57385E-02	1.21024E-02	8.25715E-03	
	5	3.75177E-02	1.45322E-02		
	6	3.12178E-02	5.56270E-03		
	7	1.66141E-02	-2.25539E-03		
	8	4.42739E-03	-5.60537E-03		
	9	-1.26755E-03	-5.76252E-03		
	10	-1.96833E-03	-4.40834E-03		
	11	1.96594E-05	-2.93587E-03		
	12	2.53043E-03	-1.89670E-03		
	13	4.17852E-03	-1.21941E-03		
	14	4.72522E-03			
	15	4.31079E-03			
	16	3.16229E-03			
	17	1.96026E-03			
	18	9.91171E-04			
	19	3.02797E-04			

Table 1: (continued)

L	m	n 2	3	4
4	1	2.78091E-04	-1.51769E-04	-3.92841E-04
	2	-1.00084E-01	-6.66747E-02	-5.00005E-02
	3	-3.33993E-02	-1.48347E-02	
	4	1.24876E-02	8.51017E-03	
	5	2.17135E-02	8.08444E-03	
	6	1.38992E-02		
	7	4.32514E-03		
	8	-1.02604E-03		
	9	-2.14049E-03		
	10	-1.03380E-03		
	11	5.08078E-04		
	12	1.56959E-03		
	13	1.84922E-03		
	14	1.61271E-03		
5	1	-1.12843E-04	-1.58676E-04	-2.11585E-04
	2	-8.32400E-02	-5.55536E-02	
	3	-2.38350E-02		
	4	9.97915E-03		
	5	1.37120E-02		
	6	6.81922E-03		
	7	7.81005E-04		
	8	-1.57652E-03		
	9	-1.38220E-03		
	10	-3.41975E-04		
6	1	1.17007E-04	3.06902E-05	
	2	-7.14871E-02		
	3	-1.78728E-02		

Table 1: (continued)

L	m	n 2
6	4	8.21155E-03
	5	9.23235E-03
	6	3.57675E-03
7	1	-1.65142E-04
	2	-6.23902E-02
	3	-1.38926E-02
8	1	-1.58911E-04

Table **2:** Number of terms M_{nL} needed in the (Generalized) Laguerre polynomial expansion for unit-iimplitude scatterers. (Entries left blank equal zero)

L \ n	2	3	4	5	6	7	8
1	—	—	17	7	3	2	1
2	—	17	12	3	1		
3	19	13	4	1			
4	14	5	2				
5	10	2	1				
6	6	1					
7	3						
8	1						

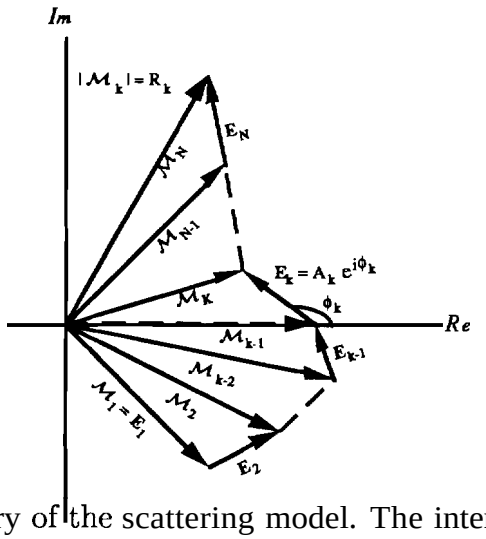

Figure 1: Geometry of the scattering model. The intensity $S_k = |\mathcal{M}_k|^2$

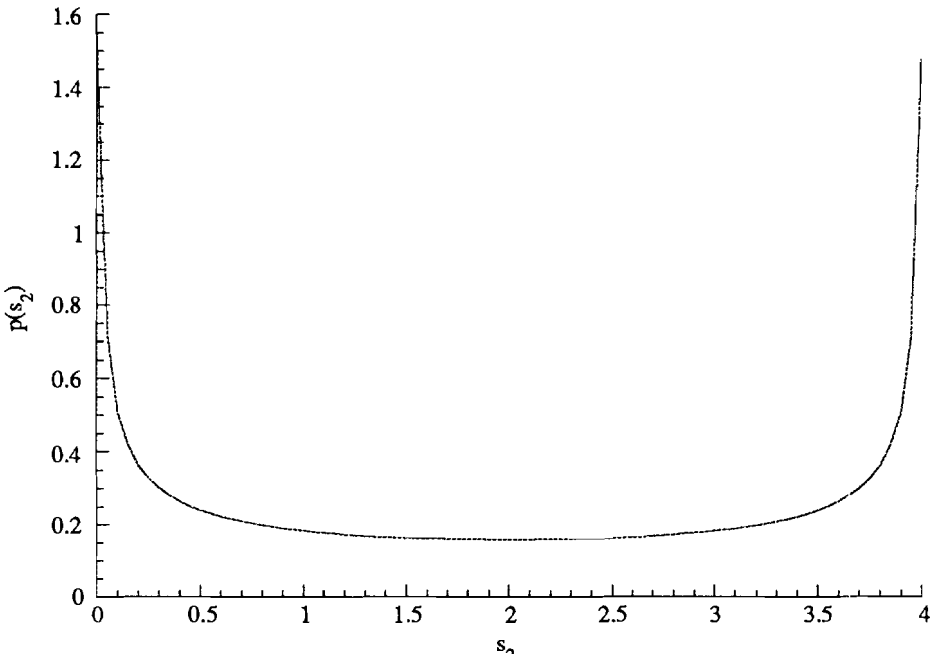

Figure **2:** Exact probability density of speckle intensity for **2** single look unit-amplitude scatterers.

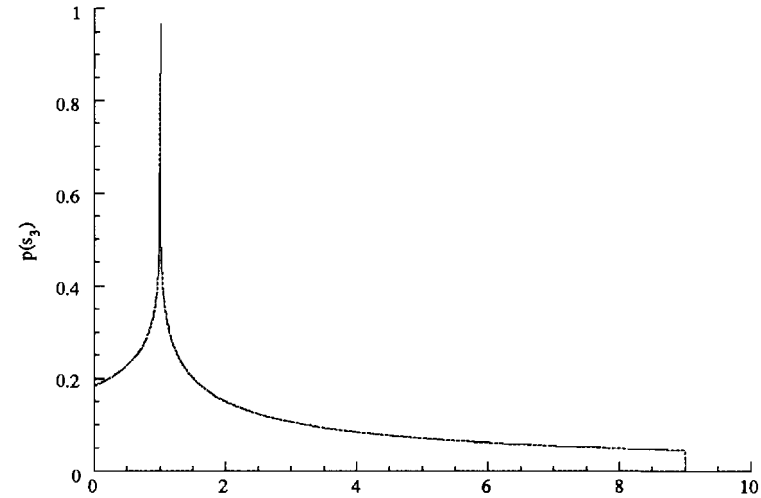

Figure **3:** Exact probability density of measured intensity for **3** single look unit-amplitude scatterers.

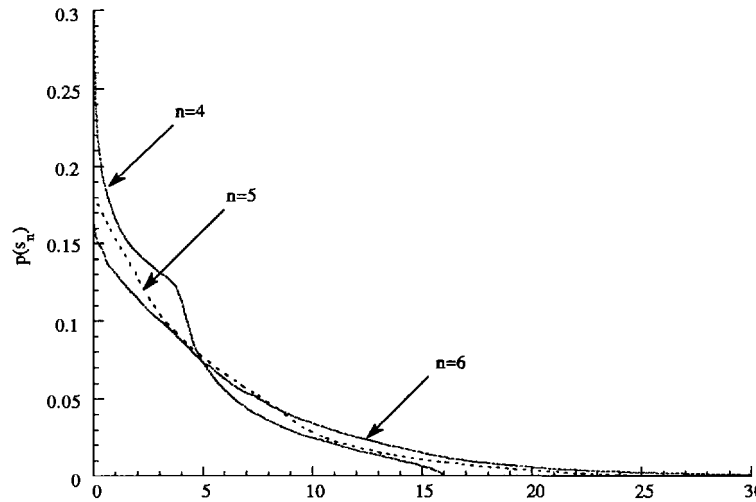

Figure 4: Exact probability density of measured intensity as the number n of unit-amplitude scatterers increases.

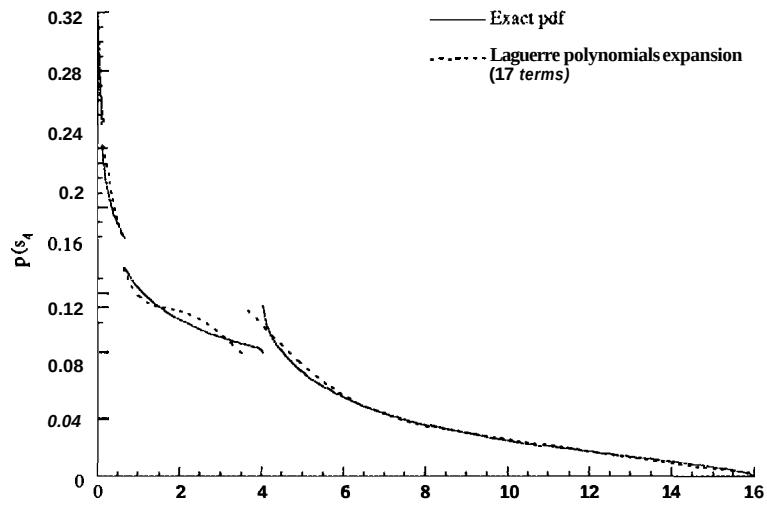

Figure 5: Exact probability density of measured intensity for 4 single look unit-amplitude scatterers vs. the Laguerre polynomial expansion. $(M_n = 17)$

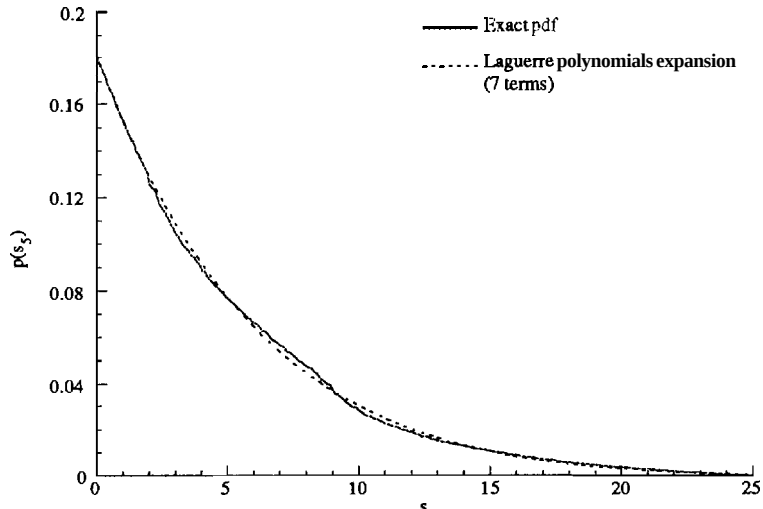

Figure 6: Exact probability density of measured intensity for 5 single look unit-amplitude scatterers vs. Laguerre polynomial expansion. $(M_n = 7)$

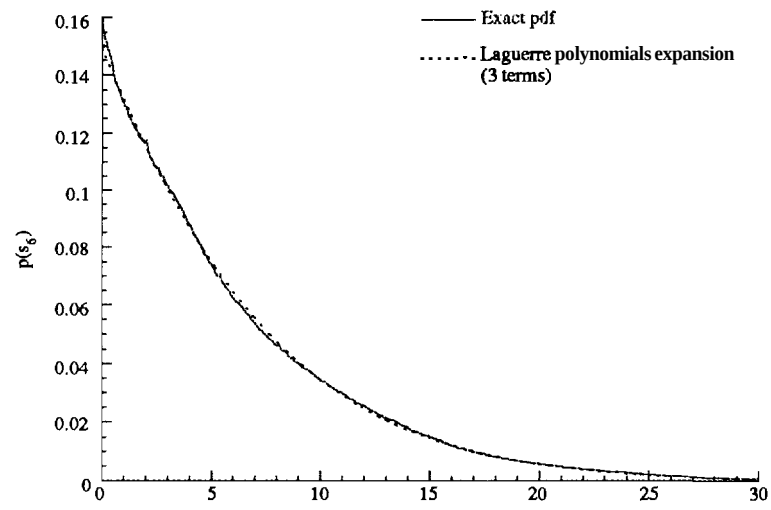

Figure 7: Exact probability density of measured intensity for 6 single look unit-amplitude scatterers vs. Laguerre polynomial expansion. $(M_n = 3)$

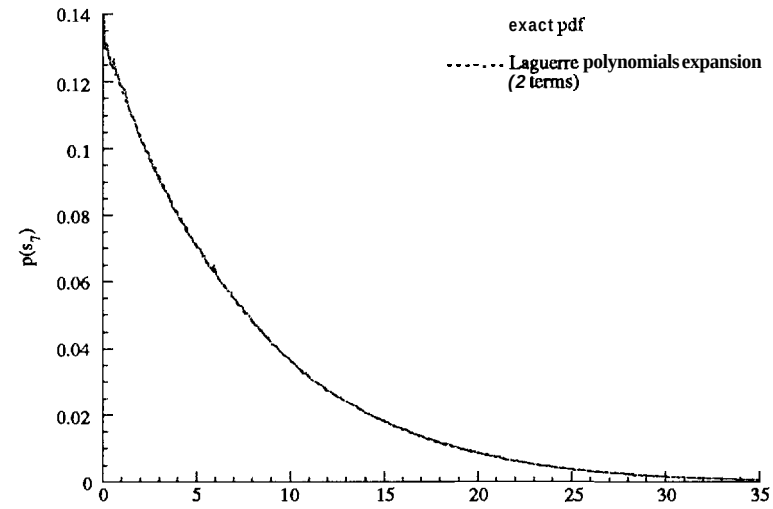

Figure 8: Exact probability density of measured intensity for 7 single look unit-amplitude scatterers vs. Laguerre polynomial expansion. $(M_n = 2)$

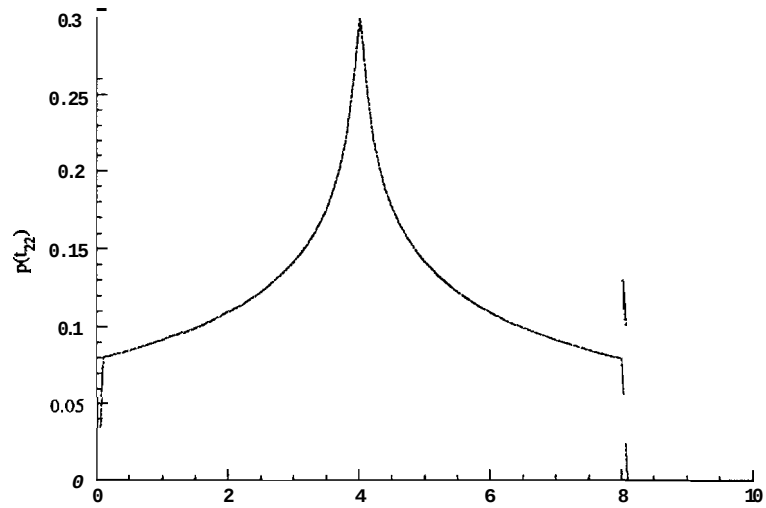

Figure 9: Exact probability density of measured intensity based on 2 looks for 2 unit-amplitude scatterers.

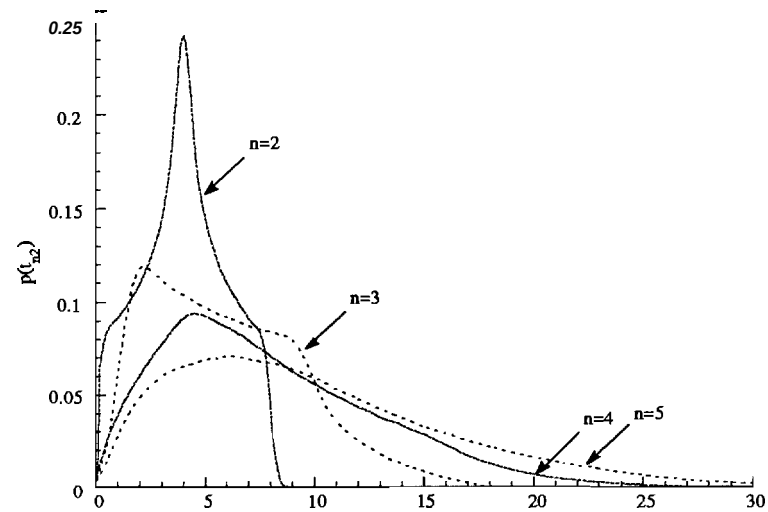

Figure 10: Estimated probability density of measured intensity for a fixed number of looks (L = 2) and various numbers n of unit-amplitude scatterers. (pdf for n = 2 and L = 2 is exact)

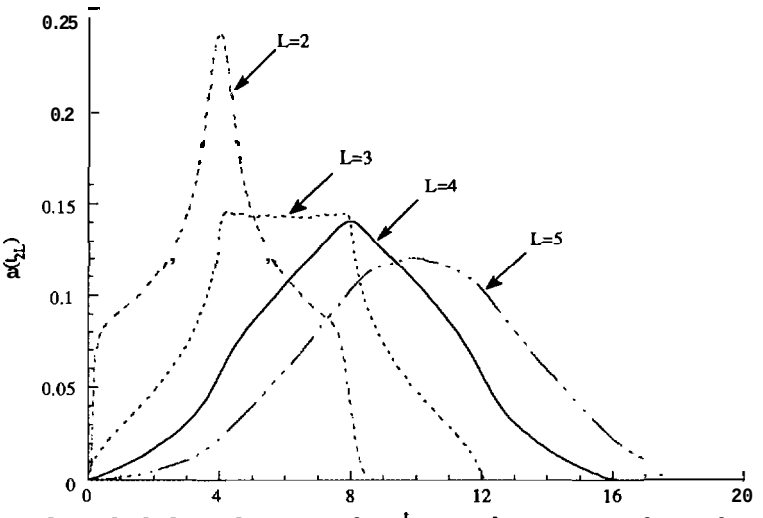

Figure 11: Estimated probability density of measured intensity for a fixed number of unit-amplitude scatterers (n = **2)** and different numbers of looks L.

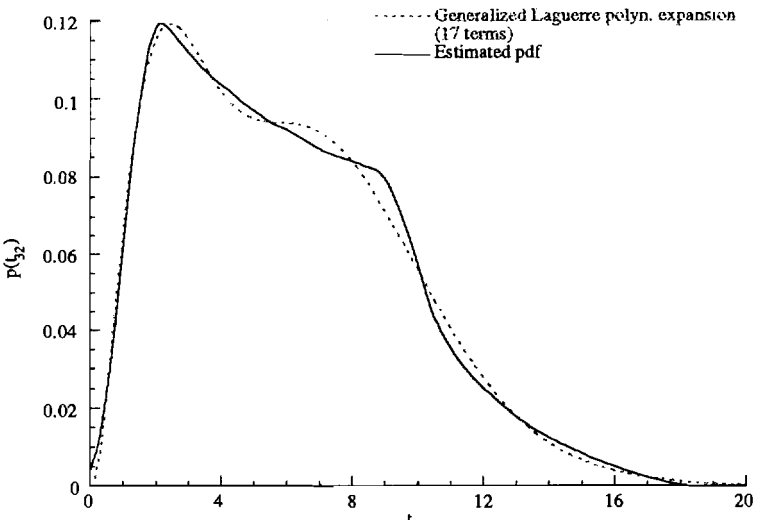

Figure 12: Estimated probability density of measured intensity for **3** unit-amplitude scatterers based on **2** looks vs. generalized Laguerre polynomial expansion. $(M_{nL} = 17)$

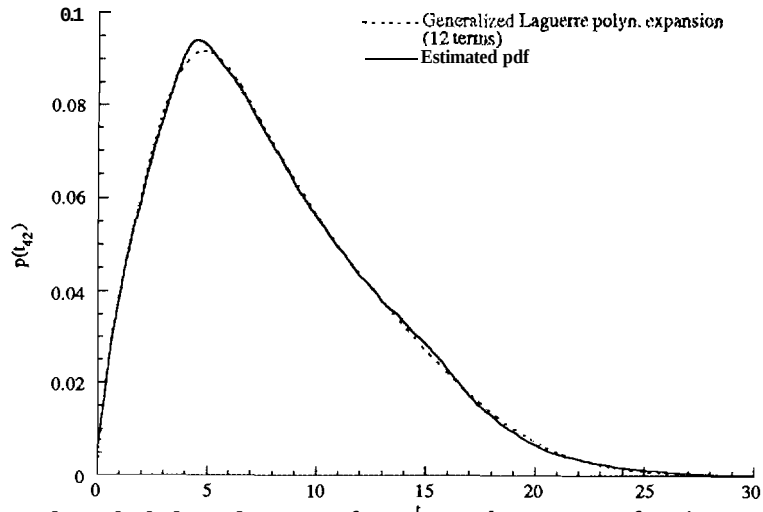

Figure 13: Estimated probability density of measured intensity for 4 unit-amplitude scatterers based on 2 looks vs. generalized Laguerre polynomial expansion. ($M_{nL} = 12$)

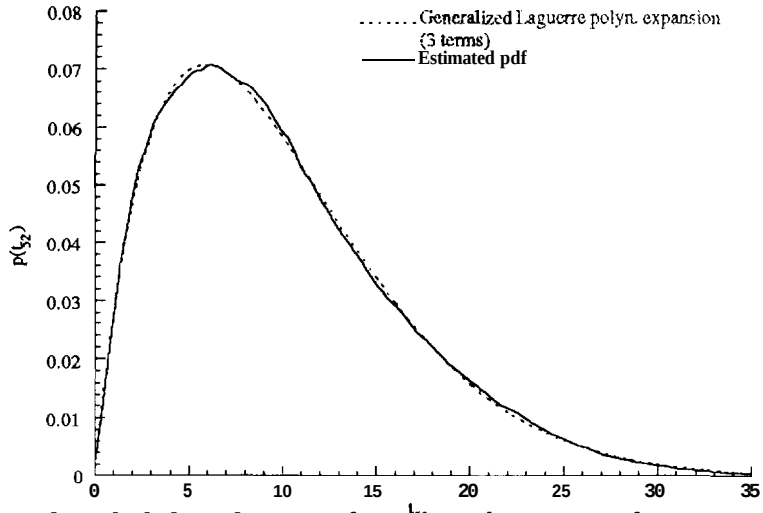

Figure 14: Estimated probability density of measured intensity for 5 unit-amplitude scatterers based on 2 looks vs. generalized Laguerre polynomial expansion. ($M_{nL} = 3$)

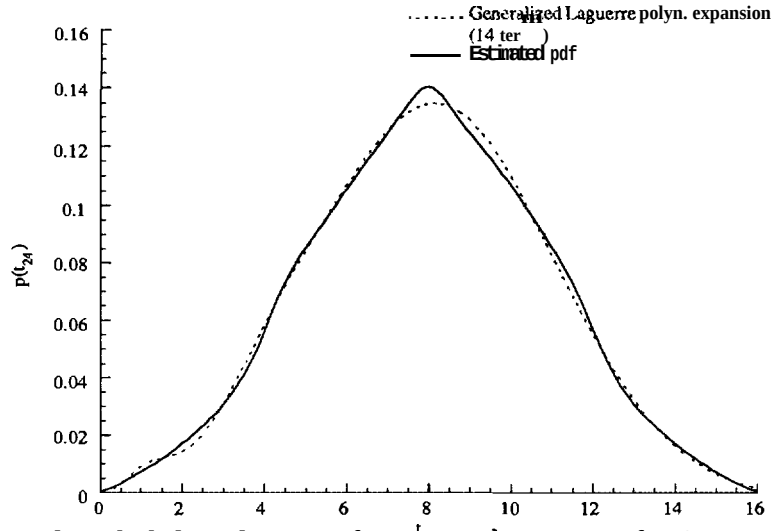

Figure 15: Estimated probability density of measured intensity for 2 unit-amplitude scatterers basecl on 4 looks vs. generalized Laguerre polynomials expansion. $(M_{nL} = 14)$

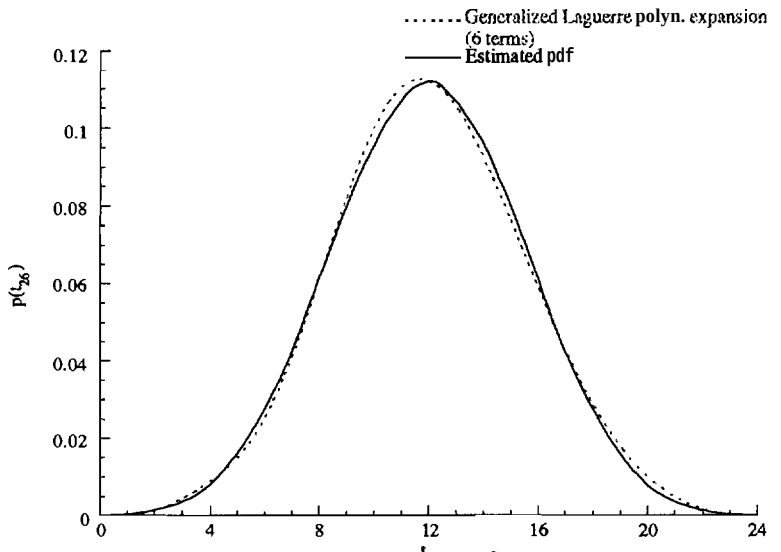

Figure 16: Estimated probability density of measured intensity for 2 unit-amplitude scatterers basecl on 6 looks vs. generalized Laguerre polynomial expansion. $(M_{nL} = 6)$

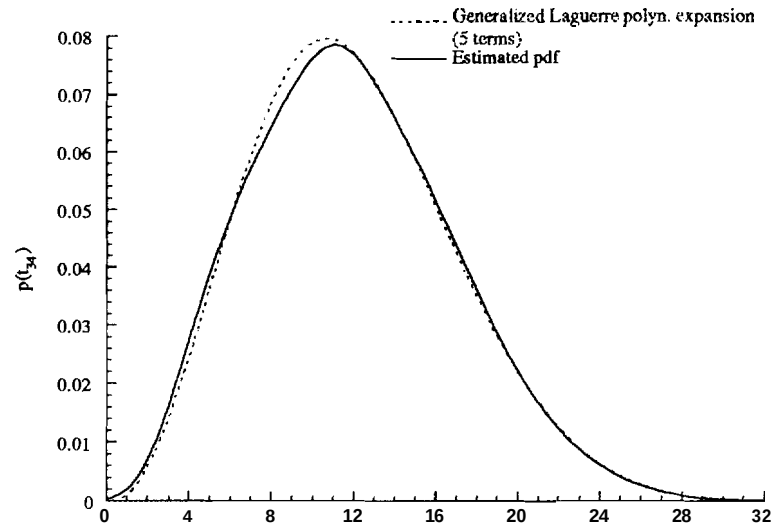

Figure 17: Estimated probability density of measured intensity for 3 unit-amplitude scatterers based on 4 looks vs. generalized Laguerre polynomial expansion. ($M_{nL} = 5$)

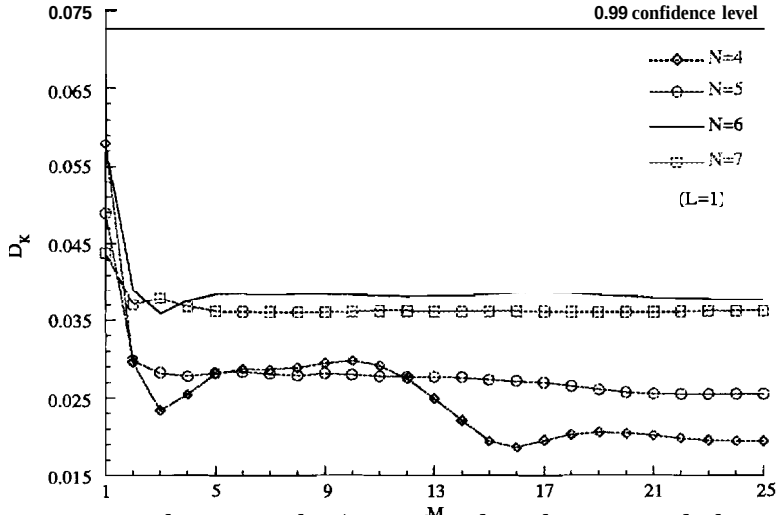

Figure 18: Distance metric between the intensity distribution and the sitmple distribution from 500 simulations as a function of the number of series terms M_n, for one look and different numbers of scatterers.

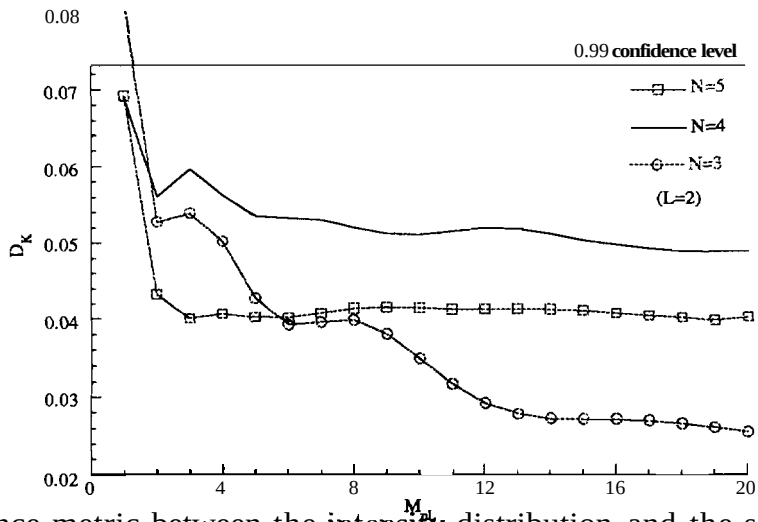

Figure 19: Distance metric between the intensity distribution and the sample distribution from 500 simulations as a function of the number of series terms M_{nL}, for **2** looks and different numbers of scatterers.

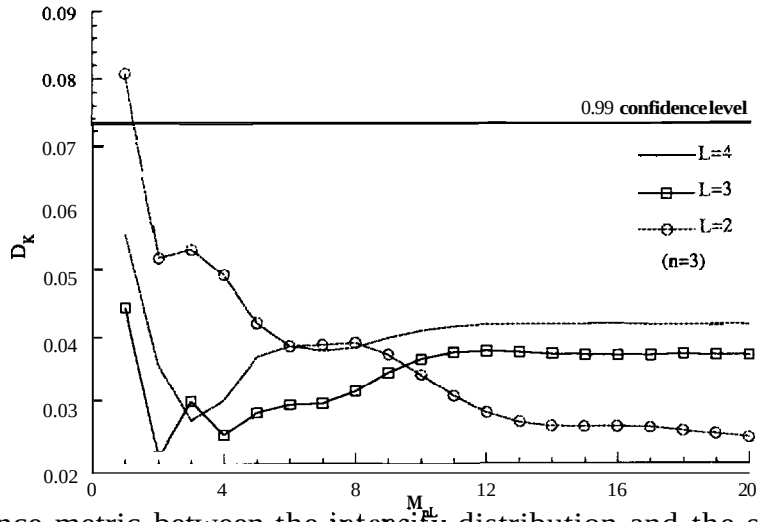

Figure 20: Distance metric between the intensity distribution and the sample distribution from 500 simulations as a function of the number of series terms M_{nL}, for **3** scatterers and different numbers of looks.